Received: 23 February 2024 | Accepted: 10 July 2024

DOI: 10.1002/bab.2644

ORIGINAL ARTICLE

WILEY

Characterization of G-quadruplexes in the *Helicobacter pylori* genome and assessment of therapeutic potential of G4 ligands

Monika Kumari[1] | **Saumya Jaiswal**[2] | **Uma Shankar**[2] | **Sharad Gupta**[2] | **Pushpangadan Indira Pradeepkumar**[3] | **Amit Kumar**[2] | **Debasis Nayak**[5] | **Vikas Yadav**[4] | **Puja Yadav**[1]

[1]Department of Microbiology, Central University of Haryana, Mahendergarh, India

[2]Department of Biosciences and Biomedical Engineering, Indian Institute of Technology Indore, Indore, Madhya Pradesh, India

[3]Department of Chemistry, Indian Institute of Technology Bombay, Mumbai, India

[4]School of Life Sciences, Jawaharlal Nehru University, New Delhi, India

[5]Department of Biological Sciences, Indian Institute of Science Education and Research (IISER), Bhopal, Madhya Pradesh, India

Correspondence
Vikas Yadav, School of Life Sciences, Jawaharlal Nehru University, New Delhi, India. Email: vikasjnu@gmail.com

Puja Yadav, Department of Microbiology, Central University of Haryana, Mahendergarh, India. Email: pujayadav@cuh.ac.in

Funding information
Indian Council of Medical Research, Grant/Award Number: VIR/21/2022/ECD-I; Ministry of Education, Scheme for Transformational and Advanced Research in Sciences, Grant/Award Number: MoE-STARS/STARS-2/2023-0373; Science and Engineering Research Board, Department of Science and Technology, Grant/Award Numbers: SERB-DST, ECR/2015/000431; Department of Biotechnology, Government of India as Ramalingaswami Fellowship, Grant/Award Number: BT/RLF/RE-ENTRY/29/2014; DST

Abstract

Helicobacter pylori, a leading human pathogen associated with duodenal ulcer and gastric cancer, presents a significant threat to human health due to increasing antibiotic resistance rates. This study investigates G-quadruplexes (G4s), which are non-canonical secondary structures form in G-rich regions within the *H. pylori* genome. Extensive research on G4s in eukaryotes has revealed their role in epigenetically regulating cellular processes like gene transcription, DNA replication, and oncogene expression. However, understanding of G4-mediated gene regulation in other organisms, especially bacterial pathogens, remains limited. Although G4 motifs have been extensively studied in a few bacterial species such as *Mycobacterium*, *Streptococci*, and *Helicobacter*, research on G4 motifs in other bacterial species is still sparse. Like in other organisms such as archaea, mammals, and viruses, G4s in *H. pylori* display a non-random distribution primarily situated within open reading frames of various protein-coding genes. The occurrence of G4s in functional regions of the genome and their conservation across different species indicates that their placement is not random, suggesting an evolutionary pressure to maintain these sequences at specific genomic sites. Moreover, G-quadruplexes show enrichment in specific gene classes, suggesting their potential involvement in regulating the expression of genes related to

Abbreviations: CD, Circular Dichroism; COG, Cluster of orthologous; IC_{50}, Half-maximal inhibitory concentration; MTT, 3-(4,5-dimethylthiazol-2-yl)-2,5-diphenyl tetrazolium bromide; NMR, Nuclear Magnetic Resonance; ORF, Open reading frame; PGQs, Putative G4 forming sequences; RBCs, Red blood cells; TSP, 3-(Trimethylsilyl) propionic-2,2,3,3-D4 acid sodium salt; UTRs, Untranslated regions.

FIST-II, Grant/Award Number: SR/FST/LSII-046/2016(C); UGC-Start-up grant from University Grant Commission, Grant/Award Number: 30-553/2021 (BSR); DBT BUILDER, Grant/Award Number: BT/INF/22/SP45382/2022

cell wall/membrane/envelope biogenesis, amino acid transport, and metabolism. This indicates a probable regulatory role for G4s in controlling the expression of genes essential for *H. pylori* survival and virulence. Biophysical techniques such as Circular Dichroism spectroscopy and Nuclear Magnetic Resonance were used to characterize G4 motifs within selected *H. pylori* genes. The study revealed that G-quadruplex ligand inhibited the growth of *H. pylori*, with minimal inhibitory concentrations in the low micromolar range. This suggests that targeting G4 structures could offer a promising approach for developing novel anti-*H. pylori* drugs.

KEYWORDS
CD spectroscopy, gene regulation, G-quadruplex, hemolysis, MTT assay, NMR, virulence

1 | INTRODUCTION

Helicobacter pylori, a prominent human pathogen that impacts more than half of the global population, is categorized as a bacterial carcinogen and is linked to conditions such as duodenal ulcer and gastric cancer.[1–3] The intricate interaction between the host and *H. pylori* can lead to colonization, resulting in various gastrointestinal diseases, including chronic gastritis, peptic ulceration, gastric adenocarcinoma, and gastric mucosa-associated lymphoid tissue lymphoma.

During the process of adherence and colonization to host cells, *H. pylori* can instigate various genetic alterations, express numerous virulence factors, and initiate diverse adaptive mechanisms. Moreover, the bacterium secretes several effector proteins and toxins, enhancing its overall pathogenicity.[4] It is noteworthy that chronic infection with *H. pylori* can persist throughout an individual's life unless antimicrobial therapy is administered to eradicate the bacterium. However, emergence of increasing antimicrobial resistance in *H. pylori* has become a substantial challenge and a critical issue. Given its clinical significance and the increasing antibiotic resistance worldwide, there is a need to identify novel and highly conserved drug targets with novel mechanisms of action. This approach is crucial for expanding the repertoire of therapeutic options and addressing the challenges posed by antibiotic resistance. G-quadruplex-forming nucleic acid motifs represent a highly studied and evolutionarily conserved class of drug targets.[5,6] These motifs are abundantly present in crucial regions of genomes across a diverse range of organisms, spanning from eukaryotes and prokaryotes to viruses, protozoans, and plants.[7–12] The conservation of these structures suggests their functional significance and underscores their potential as promising targets for drug development across different biological domains. G-quadruplexes exhibit enrichment in specific genomic regions, including open reading frames (ORFs), promoters, telomeres, and untranslated regions (UTRs) of mRNA in eukaryotic organisms as well as prokaryotic organisms.[6,13–16] The specific enrichment of G-quadruplexes in critical genomic regions suggests their involvement in essential cellular functions and highlights their potential as targets for therapeutic interventions and further research.

The propensity of guanines to self-associate and form these four-stranded helical structures has been known for several decades. The stability and formation of G-quadruplexes are influenced by various factors, including cations, sequence composition, and loop length.[11,17,18] In recent years, there has been a growing body of evidence supporting the importance of G-quadruplexes as key components in cellular processes. These structures play significant roles in various biological activities, including gene regulation, transcriptional control, telomere maintenance, and other aspects of genome stability.[11] Studying these structures enhance our understanding of nucleic acid complexity and may pave the way for innovative therapeutic approaches. Although the biological role of G4 DNA is starting to be explored in various organisms, including bacterial pathogens, genome-wide scans indicate that G4s are widely distributed in bacterial genomes, playing a role during host-pathogen interaction.[8] Only a few studies have explored the significance of G4 structures in bacterial species, indicating that research in this area remains relatively understudied compared to the eukaryotic system.[19] Several prediction algorithms, such as QuadParser, G4 Hunter, QGRS Mapper, and G4P Calculator, have been developed for finding putative G-quadruplex motifs.[20–22] G4s can adopt various structures based on their sequences, and these structures can be broadly categorized into three types of topologies: parallel, antiparallel, and hybrid.

Recently, there has been a surge of interest in G-quadruplex-specific ligands designed to bind to G-quadruplex structures with high affinity. This heightened attention is attributed to their selectivity toward G4s, which enables them to either enhance or suppress biological functions regulated by G4s.[23] One of the most promising and advanced G4 ligands is CX-5461, RNA polymerase I. This ligand is under clinical trials (Phase I/II) with high binding selectivity and stabilizing properties to a broad spectrum of G4 structures. CX-5461 has been synthesized and identified as a potential anti-tumor agent, which shows its effectiveness against advanced cancers related to *BRCA1/2* genes, showcasing its importance in cancer research.[23] Over the past two decades, numerous small molecules interacting with both DNA G-quadruplexes and RNA G-quadruplexes have been reported.[24] In the context of malaria parasites, specific ligands targeting G-quadruplex structures, such as the bis-quinoline derivatives 360A, 3AQN, and 6AQN, have demonstrated the ability to inhibit the growth of intraerythrocytic parasites.[25] These compounds are highly selective for G-quadruplex regions with a reported selectivity for *c-MYC*, 5′-UTR, and telomeric G-quadruplex.[26–30] Importantly, these ligands exhibit minimal toxicity to human cells. This suggests that the bis-quinoline derivatives show promise as potential antimalarial agents. Such findings highlight the potential of G-quadruplex-specific ligands in the development of effective and selective therapies against malaria.

In this article, with the use of biophysical and in silico approaches, we confirmed that G- rich region within the *tyrA* (prephenate dehydrogenase), *metL* (homoserine dehydrogenase [HSD]), *radA* (DNA repair protein RadA), *pbp1A* (penicillin-binding protein), *HpSCADH* (SDR family oxidoreductase), and *obgE* (GTPase ObgE) gene of *H. pylori* forms parallel and mixed G-quadruplex topology. Moreover, based on the results of an antibacterial assay, G4-specific ligands exerted an antibacterial effect toward *H. pylori* infection. Intriguingly, the G4 ligand, 360A, has shown no toxicity toward red blood cells (RBCs).

2 | MATERIALS AND METHODS

2.1 | Genomic sequence retrieval and bioinformatic analyses

The entire genome sequence of *H. pylori* (strain 26695) (NCBI Reference Sequence: NC_000915.1) was obtained in FASTA format (https://ncbi.nlm.nih.gov/nuccore/NC_000915.1?report=fasta&to=1667867). G-quadruplex sequences within *H. pylori* 26695 genome were identified through the web-based QGRS mapper (quadruplex forming G-Rich sequences) algorithm (https://bioinformatics.ramapo.edu/QGRS/analyze.php), aimed at detecting putative G4 forming sequences within ORF and intergenic regions.[31] The analysis parameters included a maximum QGRS length of 40 nucleotides, a minimum G-group size of 3, and a loop size range from 0 to 15. These parameters were chosen for their potential to generate stable G4 secondary structures.[31] Utilizing the G-score, the likelihood of G-quadruplex formation was assessed for both the sense and antisense strands. The resultant data from the QGRS mapper comprised nonoverlapping and overlapping G4s identified from both positive and negative strands (Supporting Information Table).

2.2 | Positional mapping

The G4 sequences acquired using the QGRS mapper were positioned within the *H. pylori* genome. To annotate the functionality of G4s, the GenBank database's graphical mode available on NCBI was used. Those within the coding sequences (cds) were labeled as ORFs, whereas those located between the cds were identified as intergenic G4 motifs.

2.3 | Clusters of orthologous groups (COG) functional enrichment

Regulon genes were classified based on their annotated Clusters of orthologous groups (COG) category, as outlined by Tatusov et al. (2000).[32] The G4 motifs obtained from the QGRS mapper in the target genes were examined for functional enrichment of COG categories using NCBI-BLAST (https://www.ncbi.nlm.nih.gov/research/cog/#) (Supporting Information Table).

2.4 | Biophysical characterization

2.4.1 | Circular dichroism (CD) spectroscopy

Oligonucleotides (Table 1) were sourced from IDT. However, the G-quadruplex interacting ligands (3AQN, 6AQN, and 360A) utilized in this study were prepared as previously reported.[33] Circular dichroism (CD) spectra were recorded using a Jasco J-815 Spectropolarimeter (Jasco Hachioji). Oligonucleotides (20 μM each) were prepared by heating at 95°C for 5 min and gradually cooling them to room temperature in the presence of 10 mM Tris buffer containing 50 mM each of K^+ and Na^+ ion. CD spectra profiles for each putative G-quadruplexes were captured

TABLE 1 Oligonucleotide sequences used in this study.

Sr. No.	Oligonucleotide sequences	Gene name/Locus tag
1.	5′ **GGG**CTTAT**GGGGGGG**AGTTTA**GGG** 3′	*tyrA*/HP_RS06815
2.	5′ **GGG**CTTGT**GGG**TTTA**GGG**TGTGT**GGG** 3′	*metL*/HP_RS04010
3.	5′ **GGGGGGG**AGTCCT**GGGGTGGGG** 3′	*radA*/HP_RS01095
4.	5′ **GGGG**ATGATAAGTT**GGGGG**TTAAGGTAGT**GGGGGTGGGGG** 3′	*pbp1A*/HP_RS02945
5.	5′ **GGGG**AT**GGGTGGG**TATTTTT**GGG** 3′	*HpSCADH*/HP_RS01750
6.	5′ **GGGGG**CAA**GGGGGGG**TTA**GGG** 3′	*obgE*/HP_RS01495

over the wavelength range of 220–320 nm, employing a scanning speed of 20 nm/min at 25°C. Each spectrum was accumulated in triplicate, and subsequent analysis relied on averaging the absorbance values. In all experiments, the CD spectrum of the blank (buffer) was subtracted from the CD spectra recorded for oligonucleotides. The CD spectrophotometer data were plotted and analyzed using the Origin Lab program.[5,6]

2.4.2 | Nuclear Magnetic Resonance (NMR) spectroscopy

The 1D ^{1}H-nuclear magnetic resonance (NMR) experiments were conducted using an AVANCE 500 MHz BioSpin International AG, equipped with a 5 mm broadband inverse probe. The data acquired were further processed and analyzed using Topspin software (version 1.3). 3-(Trimethylsilyl) propionic-2,2,3,3-D4 acid sodium salt served as the reference compound. A standardized concentration of 200 μM for all selected oligonucleotides was used, and experiments were carried out in a 90/10% H_2O/D_2O mixture at 298 K, utilizing a 20-ppm spectral width in 1× potassium phosphate buffer (with a 50 mM KCl concentration). The experiments were conducted in triplicate, and the average values from these three experiments were utilized for analysis.[5,6]

2.5 | *H. pylori* strain, media, and growth conditions

The *H. pylori* strain was cultured in brain heart infusion media (BHI, Becton–Dickinson) supplemented with 10% (v/v) fetal bovine serum (Gibco). The culture medium contained a combination of antibiotics: 10 μg/mL vancomycin, 5 μg/mL cefsulodin, 5 μg/mL trimethoprim, and 5 μg/mL amphotericin B, all obtained from Himedia. Additionally, 0.4% (v/v) BBL IsoVitaleX enrichment medium (Becton, Dickinson and Company) was added, and culture was maintained under microaerophilic conditions at 37°C for 48 h in presence of 5% CO_2. All antibiotics were prepared and diluted according to the guidelines outlined by the Clinical and Laboratory Standards Institute.[34]

2.6 | Antimicrobial effects of G4 ligands on *H. pylori*

To assess bacterial cell viability in the presence of G4-specific ligands, the MTT (3-(4,5-dimethylthiazol-2-yl)-2,5-diphenyl tetrazolium bromide) assay was conducted following the methodology described by Mosmann (1983) with modifications proposed by Wang et al. (2010).[35,36] *H. pylori* cells were centrifuged at 10,000 rpm for 3 min, and the resulting cell pellet was adjusted to 0.01 OD_{600} in BHI broth for each well in a 96-well plate. G-quadruplex-specific ligands (360A, 3AQN, and 6AQN) were used at concentrations ranging from 20 μM down to 0.625 μM. *H. pylori* cultures were then incubated with different concentrations of G4 ligands at 37°C for 48 h under microaerophilic conditions to assess their cytotoxic or antibacterial effects. The MTT reduction reaction was initiated by adding 10 μL of 5 mg/mL MTT stock solution to each well, followed by incubation at 37°C in the absence of light for 3 h. Later, the formazan crystals generated by the bacterial cells settled at the bottom were dissolved by using 100 μL/well of DMSO. Subsequently, the absorbance of formazan products was measured at 570 nm using a microplate reader (Synergy H1, BioTek Instruments). Cell viability was quantified by dissolving MTT in DMSO and expressing it as a percentage relative to the control group (set as 100%), which consisted of wells without any G4 ligand treatment. The inhibition rate of bacterial viability at various concentrations was evaluated based on absorbance readings. The half-maximal inhibitory concentration (IC_{50}) value was estimated using the nonlinear log inhibitor versus normalized response—variable slope least squares fit algorithm available in GraphPad Prism 5.0.

2.7 | Hemolysis analysis

To evaluate the potential hemolytic activity of G-quadruplex specific ligand (360A) on human erythrocytes,

erythrocyte hemolytic assay was followed as described by Palermo and Kuroda.[37] In brief, human RBCs were washed three times with phosphate-buffered saline (PBS, pH 7.4) by centrifugation at 1000 rpm for 10 min at 4°C. After three washes with PBS, the RBCs were resuspended in the same buffer to attain a concentration of 3.3% (v/v). Serial two-fold dilutions of 360A (0.625, 1.25, 2.5, 5, 10, and 20 μM) were prepared in PBS and added to 90 μL of the RBC suspension in microtiter plate. Positive control involved 0.1% Triton X-100, known for inducing complete RBC lysis, whereas PBS served as the negative control. Following an incubation period of 1 h at 37°C, the microtiter plate was centrifuged at 1500 rpm for 10 min. Afterward, 10 μL of supernatant from each well of microtiter plate was transferred to a new microtiter plate containing 90 μL of PBS. The concentration range of 360A was aligned with that used for assessing the antibacterial activity against *H. pylori*. The absorbance of released hemoglobin was measured at 405 nm using a multimode microplate reader (Synergy H1, BioTek Instruments). This experiment was carried out in triplicate. The calculation of % RBC lysis for each sample was determined using the following formula:

$$\%\,\text{Hemolysis} = [(A - AO)/(AX - AO)] \times 100$$

where A is OD_{405nm} with the G-quadruplex specific ligand, AO is OD_{405nm} of the negative control (PBS), and AX is OD_{405nm} of the positive control (0.1% Triton X-100).

2.8 | Statistical analysis

All experiments were performed in at least triplicates and repeated three times, and the results shown were expressed as the mean ± standard deviation unless otherwise indicated. GraphPad Prism 5.0 (GraphPad Software) was used for statistical analysis.

3 | RESULTS

3.1 | G-quadruplex sequences are predominantly situated in the open reading frame (ORF) regions

To investigate the distribution and occurrence of PGQs motifs in the *H. pylori* genome, we conducted a computational screening of *H. pylori* genome using QGRS mapper. We identified a total of 255 non-overlapping and 2541 overlapping G-quadruplex (G4) motifs on both the positive and negative strands. Out of the 255 nonoverlapping PGQs, 128 were located on the sense strand and 127 on the antisense strand. In the case of the 2541 overlapping PGQs, 1200 were identified on the sense strand and 1341 on the antisense strand (Figure 1A, Supporting Information Table). For further studies, we focused on 255 nonoverlapping G4 motifs and performed further analysis. Subsequently, positional mapping of G4 sequences elucidates the nonrandom distribution of G4 sequences in the *H. pylori* genome. Our observation revealed that approximately 7.031% (9) of G4 motifs were present in intergenic regions, and 92.96% (119) of G4 motifs were in ORF regions of nonoverlapped positive strand. However, 5.52% (7) of G4 motifs in intergenic and 94.48% (120) of G4 motifs in ORF region of nonoverlapped negative strand were observed. Overall, 6.27% (16) of G-quadruplex (G4) sequences were found in the intergenic regions combining sense and antisense strands. Conversely, around 93.73% (239) of G4 sequences were located within the ORFs of various protein-coding genes (Figure 1B).

3.2 | Functional analysis of *H. pylori* G4 motifs

To gain a more comprehensive understanding of the position of G4 motifs within specific gene classes, functional clustering was performed for G-rich sequences identified in ORF regions (93.7%) using functional COG analysis. Out of 239, only 215 genes could be assigned to functional categories, while the rest did not find a significant hit with the COG database. In the COG category assignment, a notable enrichment of G-quadruplex (G4) sequences was observed in genes associated with cell wall/membrane/envelope biogenesis (M) and amino acid metabolism (E), whereas poorly characterized categories (R and S) exhibited a lower occurrence of G4 motifs. Further analysis delved into the distribution of G4 motifs within genes involved in cell wall/membrane/envelope biogenesis, revealing that 21.8% of G4 sequences were identified on the sense strand, whereas 16.6% of G4-containing genes were located on the antisense strand. Additionally, when exploring the occurrence of G4 sequences in genes related to amino acid transport and metabolism categories, we found that 11.7% of G4 sequences were present on the sense strand, and 8.33% of G4-containing genes were situated on the antisense strand. The abundance of the G4 motifs in genes belonging to COG category of cell wall/membrane/envelope biogenesis in *H. pylori* is correlated with the high prevalence of outer membrane vesicles and outer membranes in these bacteria (roughly 4% of their genes), which are specifically allocated to the encoding of outer membrane proteins (OMPs). Conversely, other COG categories (J, L, D, V, T, N, Z, W, U, O, X, C, F, H, I, P, Q, R, and S) exhibited G-quadruplex (G4) motif occurrence below 9% (Figure 2). This comparison provides insights into the distribution of G4 motifs across different functional categories in the *H. pylori* 26695 genome.

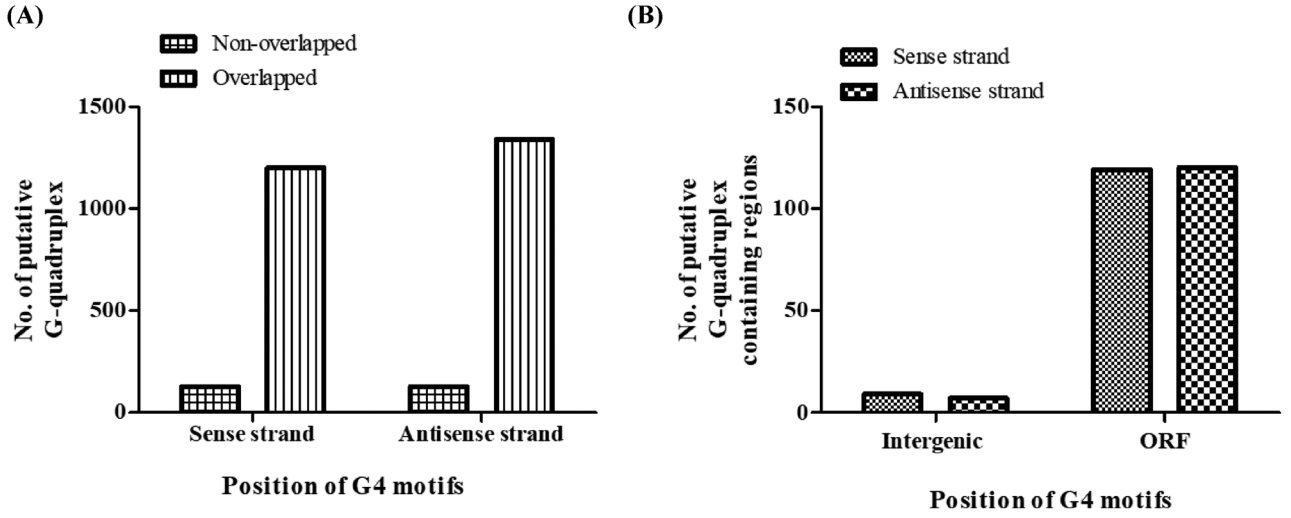

FIGURE 1 (A) The number of G-quadruplex motifs, containing nonoverlapping and overlapping sequences, in both sense and antisense strands. (B) The number of putative G-quadruplex containing regions present in the open reading frames and intergenic regions in both sense and antisense strands.

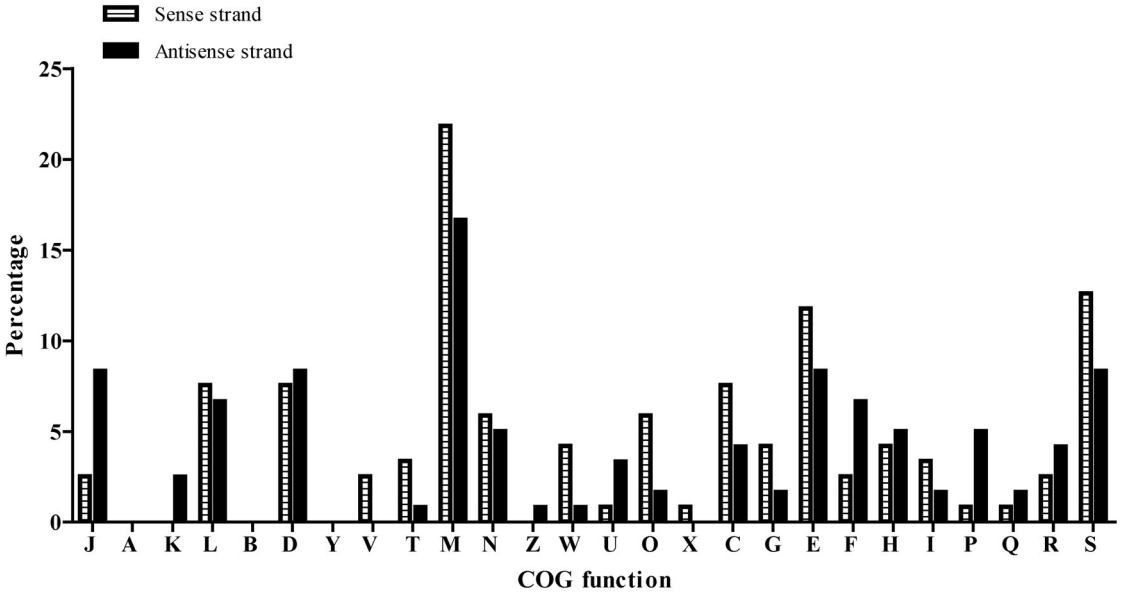

FIGURE 2 The comparison of Clusters of orthologous groups (COG) function categories of genes based on occurrence and distribution of G-quadruplex (G4) motifs present in *H. pylori* 26695 is illustrated on the vertical coordinate, representing the percentage of the G4 motifs within each COG category relative to the total number of functional genes. The COG designations are as follows: J—translation, ribosomal structure, and biogenesis, K—transcription, L—replication, recombination, and repair, D—cell cycle control, cell division, chromosome partitioning, T—signal transduction mechanisms, M—cell wall/membrane/envelope biogenesis, N—cell motility, U—intracellular trafficking, secretion, and vesicular transport, O—posttranslational modification, protein turnover, chaperones, C—energy production and conversion, G—carbohydrate transport and metabolism, E—amino acid transport and metabolism, F—nucleotide transport and metabolism, H—coenzyme transport and metabolism, I—lipid transport and metabolism, R—general function prediction only, S—function unknown.

3.3 | G-rich sequences adopt parallel and hybrid topologies of G-quadruplexes (G4)

We determine the ability of these 6 selected G4 sequences identified from the QGRS mapper to form G quadruplexes in vitro. CD was performed in the presence of both K^+ and Na^+ ions to determine the G4 formation and topology. Salt concentrations of 50 mM (K^+ and Na^+) were chosen to mimic eukaryotic physiological conditions. All the selected G4 sequences displayed CD signals indicative of G4 formation. The G4 sequences present in *tyrA*, *radA*, *pbp1A*, *HpSCADH*, and *obgE* genes exhibited a

characteristic CD spectrum with a positive peak at 260 nm and a negative peak around ~240 nm, indicative of a parallel G4 conformation.[5] In contrast, the CD spectra of the G4 sequence within the *metL* gene displayed two positive peaks at ~260 and ~290 nm, along with a negative peak at ~240 nm, characteristic of a mixed confirmation (Figure 3A). To further confirm the formation of G quadruplexes by these G-rich sequences, ^{1}H imino proton NMR analysis of G-rich sequences of gene *tyrA, metL, radA*, *pbp1A*, *HpSCADH*, and *obgE* oligonucleotides was performed. The ^{1}H NMR spectra of these genes, except *obgE*, exhibited signals between 11.0 and 12.0 ppm, which is indicative of the presence of imino protons of guanine residues in G-quartets.[5] However, signals detected in the range of δ 12.5–13.3 ppm imply the creation of Watson-Crick GC base pairs. In the NMR spectra of all oligonucleotides except *obgE*, signals appeared within the range of δ 10.5–12.5 ppm, suggesting the potential formation of G4 structures in *tyrA*, *metL*, *radA*, *pbp1A*, and *HpSCADH* oligonucleotides (Figure 3B). On the other hand, the absence of a peak in this region in the NMR spectrum of *obgE* suggests the absence of a G-quadruplex topology, and thus, the absence of G4 structures in this oligonucleotide.

3.4 | Antibacterial activity of G4 ligands

G4 ligands, previously identified for their antimalarial properties, were screened against *H. pylori* to explore their antibacterial potential, revealing 360A as a promising lead candidate. The antimicrobial activity of G4 ligands (360A, 3AQN, and 6AQN) was assessed through MTT assay. The chemical structure of these compounds shown in Figure 4 exhibited significant antibacterial activity against *H. pylori*. In vitro, the cytotoxicity activity of these G4 ligands was measured against *H. pylori* cells at different concentrations (0.625, 1.25, 2.5, 5, 10, and 20 μM). The antimicrobial activity of 360A showed an IC_{50} value of ~15.48 μM ($\log_{10}$ IC_{50} = 0.07816 μM) on *H. pylori* cells, indicating a detrimental impact of the G-quadruplex-specific ligand 360A on *H. pylori* cell viability (Figure 5A). However, no cytotoxic effect was observed against *H. pylori* when treated with 3AQN or 6AQN (Figure 5B,C).

3.5 | 360A exhibits non-cytotoxic effects on red blood cells (RBCs)

The initial assessment of cellular toxicity often involves the Hemolysis assay. The hemolytic activity of 360A was examined in erythrocytes, and the subsequent release of hemoglobin was utilized to assess the hemolytic activity across a concentration range of 0.625–20 μM. At its highest concentration (20 μM), 360A demonstrated minimal lysis, and all tested concentrations of 360A exhibited hemolysis < 20%, indicating a higher tolerance of human erythrocytes for 360A (Figure 6). These collective findings support the characterization of 360A as having relatively low hemolytic activity, reinforcing its characterization as benign toward human RBCs.

4 | DISCUSSION

In recent years, non-canonical secondary structures known as G-quadruplex structures have been identified in nearly all organisms, including bacteria and thus have been considered potential targets for antibacterial strategies. The identification of G-quadruplex motifs in the genomes of human pathogens has been shown to influence the regulation of genes they harbor, consequently altering their pathogenicity. Therefore, identification and determining the genomic distribution of G-quadruplexes (G4s) are essential. Since the bacterial genome encodes proteins using both strands, our analysis extended to examining the presence of G-quadruplex motifs in both the sense and antisense strands of the bacterial genome. In our investigation, we employed an in silico approach to scrutinize the *H. pylori* genome. Using the criterion of G-tract ≥3 and loop length ≤15, we detected almost equal number of G-quadruplex motifs in both the positive or non-template strand and negative or template strand of the *H. pylori* genomes, indicating the absence of significant strand biases. Similarly, in warm-blooded animals, G-quadruplex motifs are prevalent on both the template and non-template strands.[38–42] However, in other organisms, the formation of these exceptionally stable structures is more effective on the non-template strand, displaying a noticeable strand bias. G4 motifs on the non-template strand may hold greater significance as they prompt transcription reinitiation and positively influence gene expression. Conversely, on the template strand, they may impede transcription by causing RNA polymerase stalling, potentially exerting a negative impact.

Across various plant species, G3-type parallel G-quadruplexes were commonly observed in intergenic regions, whereas G2-type parallel G-quadruplexes predominantly appeared in genic regions. This pattern implies a non-random distribution and suggests potential involvement in various cellular processes. According to a recent study, a non-random localization of G4 was seen within the nuclear and mitochondrial genomes of *Saccharomyces cerevisiae*.[43] Moreover, non-randomization was observed by another group in Deinococcus-Thermus, where G4 was seen in ncRNA and mRNAs, as well as in tRNAs and regulatory regions.[44] Similarly, in the *H. pylori*

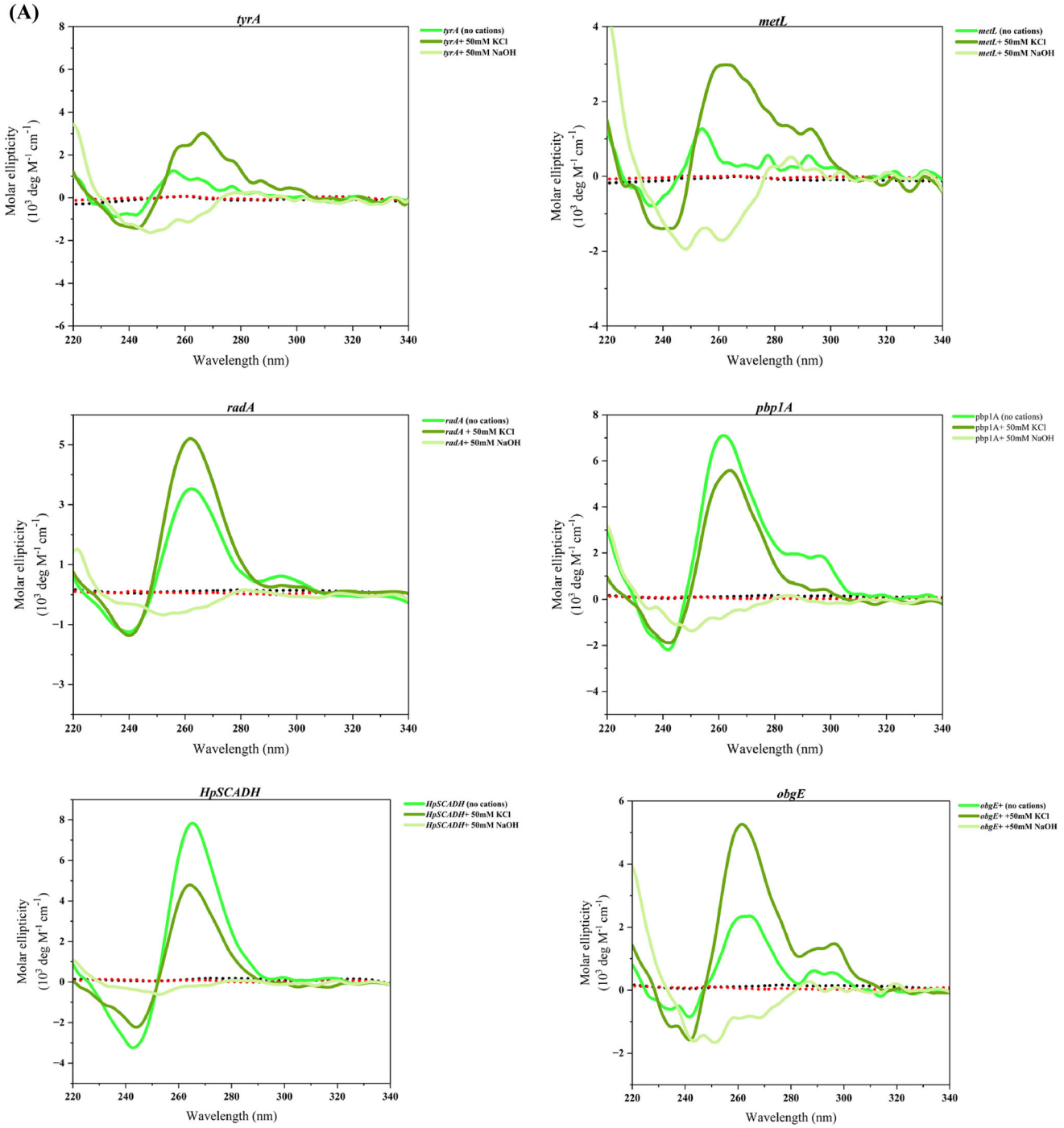

FIGURE 3 (A) CD spectra were obtained for the oligonucleotides *tyrA, metL, radA, pbp1A, HpSCADH*, and *obgE* in the presence of both K^+ and Na^+ ions. Following the addition of KCl, the CD spectra of the *metL* oligonucleotide exhibited a positive peak at 290 nm with a shoulder at 260 nm and a negative peak at 240 nm, indicating the formation of a G-quadruplex structure with a hybrid-type conformation. In contrast, oligonucleotides containing *tyrA, radA, pbp1A, HpSCADH*, and *obgE* sequences predominantly adopted a parallel conformation. The data from the graphs revealed significant differences between the CD spectra of oligonucleotides in the presence of Na^+ and K^+ ions, highlighting enhanced stability of G4 sequences specifically with K^+ ions. (B) The imino region within the 1D ^{1}H spectra of oligonucleotide samples (*tyrA, metL, radA, pbp1A*, and *HpSCADH*) was examined. The chemical shift falling between 10 and 12 ppm in the 1D ^{1}H nuclear magnetic resonance (NMR) spectra indicates the existence of imino-proton groups in five illustrated PGQs.

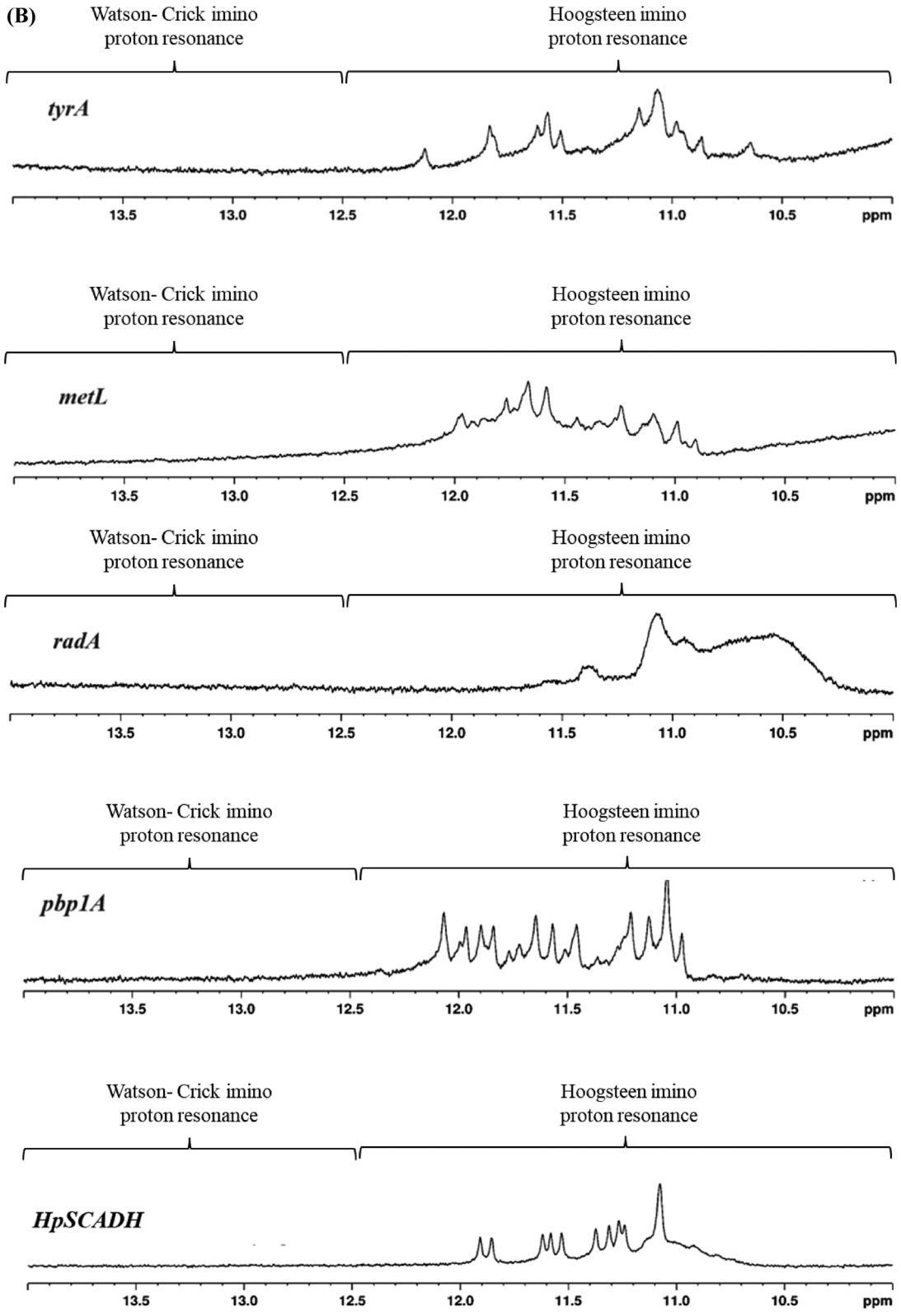

FIGURE 3 Continued

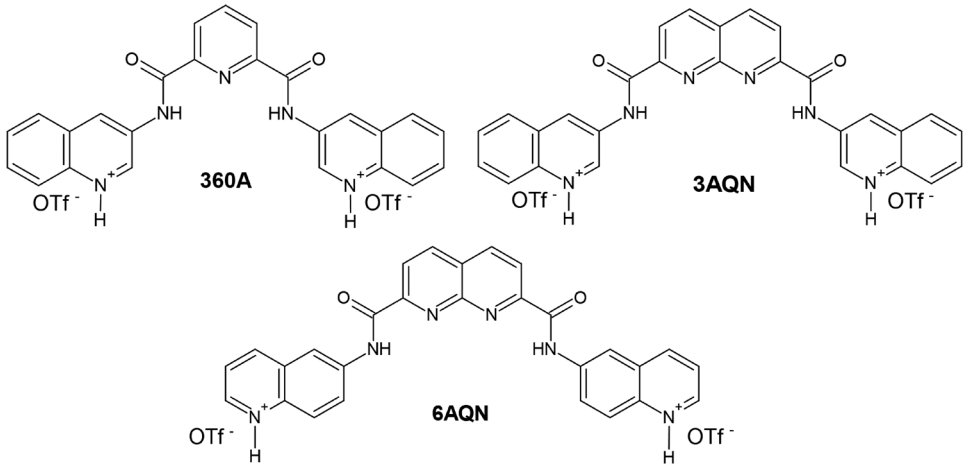

FIGURE 4 Chemical structure of G-quadruplex specific ligands 360A, 3AQN, and 6AQN.

26695 strain, about 93.7% of G3-type G-quadruplexes were identified in ORFs of protein-coding genes, and approximately 6.2% were located within the intergenic regions. This distribution aligns with the findings observed in plants. These findings highlight the distinct and non-random localization of G4-forming sequences in bacterial genomes, providing further support from previous research.[44] To gain a more thorough understanding of the distribution and prevalence of G4 motifs in specific gene classes, we performed positional mapping and conducted functional analysis using COG. Despite *H. pylori* having an average G + C content of 39%, our analysis has revealed an enrichment of G4s in the genes associated with cell wall/membrane/envelope biogenesis (M) as well as amino acid transport and metabolism (E) within its genome. Several studies have identified genes associated with M (membrane) and E (energy) functions as potential targets for novel drug development.[45–47] As a result, our research corroborates these observations, revealing the highest concentration of G4 motifs within the COG functional category M. The M category encompasses genes responsible for regulating OMPs, lipopolysaccharide (LPS) synthesis, lipoprotein-related proteins, penicillin-binding proteins in the cell wall, and proteins involved in cell division.[48] According to the report by Yang et al. (2021), COG category M includes genes, such as *flgM*, *flgR*, *flhB*, *flhB2*, *fliF*, *fliM*, *fliQ*, *babA/hopS*, *futA*, *futB*, *galE*, and *ureB*. Among these, genes essential for the structure and function of flagella include *flgM*, *flgR*, *flhB*, *flhB2*, *fliF*, *fliM*, and *fliQ*. The BabA protein facilitates adhesion to host cells, is encoded by the babA/hopS gene, and crucial for *H. pylori's* colonization. Fucosyltransferases, encoded by *futA* and *futB*, are linked to LPS structure, which also contributes to virulence. Another gene involved in LPS synthesis is *galE*. Additionally, *ureB* encodes the UreB (urease beta subunit) protein, essential for neutralizing gastric acidity, aiding *H. pylori's* survival.[49] In a study by Kumar et al. on *H. pylori* from Malaysia, an enrichment of genes related to cell wall biosynthesis and transport of amino acids and ions was observed in the core genome. This enrichment of transport-related genes highlights the bacteria's reliance on host metabolites, influenced by its long-term interaction with the host.[50] This enrichment strongly suggests the essential role of these genes in *H. pylori's* survival and virulence.

The observed over representation of G4s emphasizes the significance of these biological processes for *H. pylori*, highlighting their importance in the bacterium's adaptation and pathogenicity.

Recently, research has shown that *H. pylori* possess conserved G4 DNA within four Nickel-transport associated genes.[6] In our study, we revealed the presence of G-quadruplex through biophysical approach in six selected genes (*tyrA*, *radA*, *pbp1A*, *HpSCADH*, *obgE*, and *metL)* of the *H. pylori* genome. The pathogenicity of *H. pylori* depends on a multitude of virulence factors. Hence, we focused on these genes known to form G-quadruplex structures, given their potential association with virulence, for further biophysical characterization. In several bacteria, RadA has been implicated in DNA repair mechanisms in association with other proteins like RecA. Interestingly, certain potential small RNAs have been predicted to bind to mRNA encoding proteins involved in radiation damage recovery, including RadA, RecA, and RuvA, in radioresistant species of the Deinococcaceae family, such as *Deinococcus geothermalis*.[51,52] *tyrA* is another gene of significance, playing a critical role in biosynthetic pathways by catalyzing the conversion of prephenate into tyrosine through a sequential, two-step process. This process relies on the action of the prephenate dehydrogenase enzyme (TyrA), aminotransferases (AroJ), and an unidentified protein involved in tyrosine biosynthesis. Notably, this entire

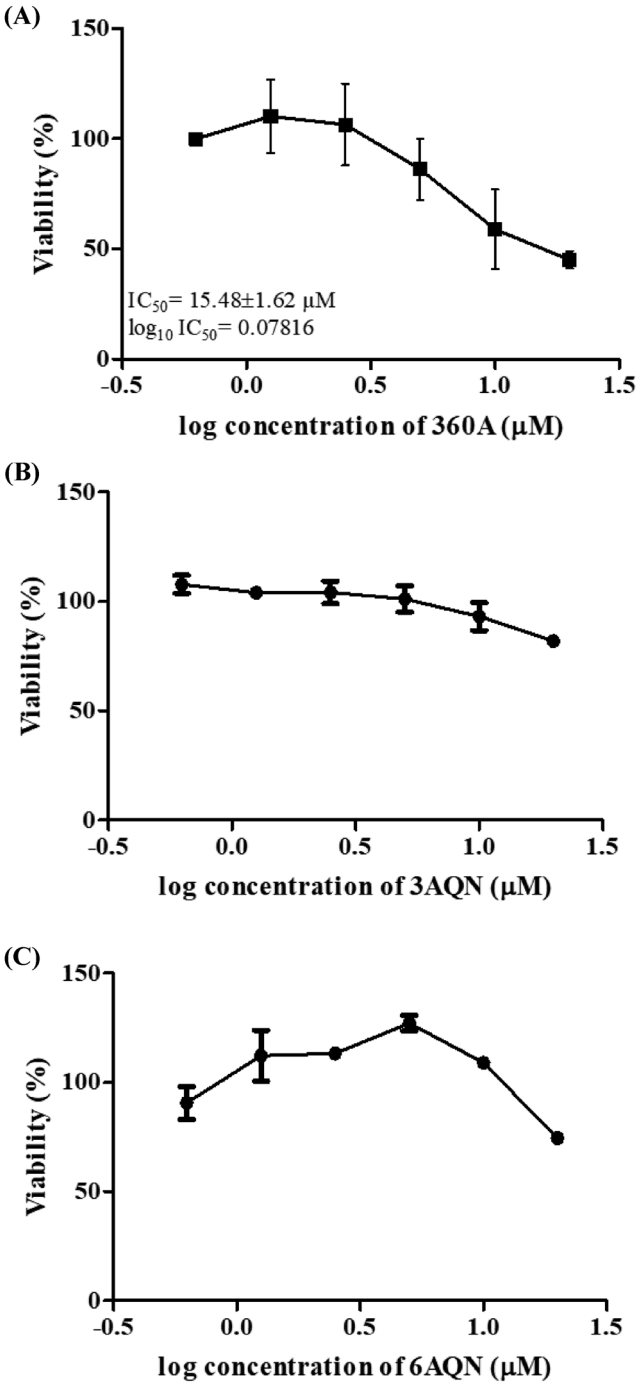

FIGURE 5 Cell viability assay. Dose-dependent effect of G-quadruplex ligands (A) 360A, (B) 3AQN, and (C) 6AQN on *Helicobacter pylori* after 48 h of cell growth.

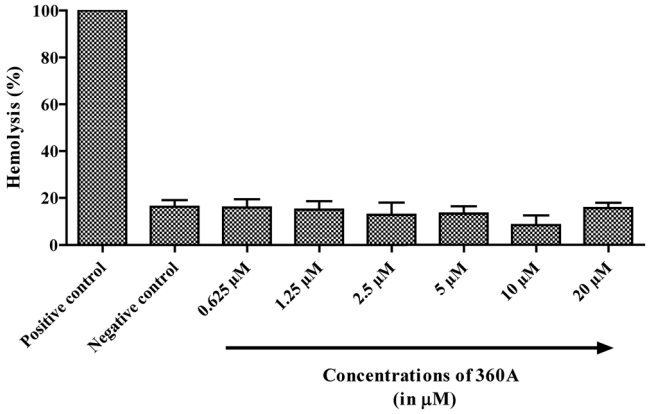

FIGURE 6 Hemolytic activity of 360A in human red blood cells. Dose response data for the hemolytic activity of 360A with concentrations ranging from 0.625 to 20 μM.

process is subject to feedback inhibition, regulating TyrA activity through the presence of tyrosine.[53,54] On the other hand, Pbp1A has attained significant attention in research due to the increasing prevalence of amoxicillin-resistant *H. pylori* strains, which poses a challenge to therapies relying on this antibiotic for eradication. Numerous studies have shown that mutations within the *pbp1A* gene correlate with amoxicillin resistance in *H. pylori*. Consequently, modifications in the *pbp1A* gene, in conjunction with mutations in the *hopC* gene and the deletion in the porin-encoding *hopB* gene of *H. pylori*, among other factors, serve as supplementary elements contributing to an elevated level of resistance in *H. pylori*.[55,56] Another gene alcohol dehydrogenases (HpSCADH) play a significant role in the generation of toxic aldehydes implicated in the pathogenesis of *H. pylori*-induced damage to the gastric mucosa. HpSCADH, a member of the cD1e subfamily of NAD+ dependent classical short-chain alcohol dehydrogenases, functions as a monomeric enzyme with a size of approximately 29 kDa. Studies have demonstrated that inhibiting HpSCADH alone with pyrazole leads to growth impairment in wild type *H. pylori cells*, mirroring the growth patterns observed in the isogenic mutant. These findings underscore the fundamental role of alcohol-metabolizing enzymes in *H. pylori*'s adaptation to acidic environments and its growth dynamics.[57] Furthermore, *metL*, which encodes HSD, serves as a crucial enzyme in the aspartic acid pathway. Its primary function involves converting L-aspartate-4-semialdehyde into L-homoserine and vice versa. Interestingly, HSD remains inactive in humans, making it an attractive target for potential therapeutic interventions. Consequently, numerous inhibitor compounds have undergone rigorous testing against this enzyme, offering promising prospects for therapeutic advancements.[58]

We have observed that most of the G4s were forming parallel G-quadruplex topology in *tyrA*, *radA*, *pbp1A*, and *HpSCADH* gene, whereas *obgE* and *metL* were showing hybrid G-quadruplex topology. On other hand, the NMR study showed that five out of six genes exhibited a chemical shift ranging from 10.5 to 12.5 ppm. This shift in the 10–12 ppm range in NMR is attributed to the imino group present in the Hoogsteen bonding of G-quadruplex DNA. These particular genes were chosen based on their significance in both virulence and biosynthetic pathways.

Collectively, CD and NMR data unequivocally confirmed the formation of these secondary structures, providing experimental validation consistent with the in silico analysis. To explore a novel therapeutic strategy for combating *H. pylori* infection, we conducted a screening of G-quadruplex (G4) ligands to assess their efficacy as antibacterial agents. This approach capitalizes on the potential of targeting quadruplex structures in guanine-rich regions of the bacterial genome, which has been proposed as a promising therapeutic target for developing antimicrobial drugs against various human pathogenic bacteria.

In the present study, we evaluated the influence of bisquinolinium derivatives of 1,8-naphthyridine and pyridine (3AQN, 6AQN, and 360A) G4 ligands on the growth of *H. pylori*. Originally identified as antimalarial agents, these ligands have shown effective inhibition of parasite growth with minimal adverse effects on human cells. Our study specifically highlights the inhibitory effect of ligand 360A on *H. pylori* growth. Cell cytotoxicity assays revealed a decrease in *H. pylori* cell viability directly correlating with increasing concentrations of 360A. Our study demonstrates that 360A has the capability to stabilize *H. pylori* G-quadruplex structures, consequently inhibiting its growth. This highlights the interaction between the established G-quadruplex binding ligand (360A) and G-quadruplex motifs. Additionally, the hemolysis assay demonstrated that even at the highest concentration (20 μM), 360A exhibited low hemolysis (below 20%). This finding suggests a relatively low hemolytic activity, confirming the relatively benign nature of 360A toward human RBCs.

Our data suggest the potential use of G4 ligand 360A as an antibacterial agent for treating *H. pylori* infection. G4 ligands exhibiting antibacterial properties hold promise as G4-targets for addressing *H. pylori* infections. However, the precise mechanism underlying the antibacterial activity has yet to be thoroughly explored.

5 | CONCLUSION

H. pylori is associated with several gastro-duodenal diseases, posing a global threat. However, no target-based treatment is available yet. Our study employs a comprehensive approach, integrating bioinformatics analysis and biophysical characterization, to explore the prevalence and potential biological significance of G-quadruplexes in the *H. pylori* genome. In conclusion, we investigated the enhanced inhibitory effect of 360A against *H. pylori*, thereby increasing its value as an antimicrobial agent. Given the important roles of G-quadruplex ligands in antibacterial activity, this study proposes the utilization of G4 ligands as a potential strategy to combat *H. pylori* infections.

AUTHOR CONTRIBUTIONS

Puja Yadav, Vikas Yadav, and Monika Kumari conceived, designed, and analyzed the experiments. CD spectroscopy and NMR was done by Monika Kumari, Saumya Jaiswal, and Uma Shankar. Other experiments were performed by Monika Kumari and Vikas Yadav. Puja Yadav, Vikas Yadav, and Monika Kumari analyzed the data and wrote the main manuscript. MS reviewed by Amit Kumar, Sharad Gupta, Debasis Nayak, and Pushpangadan Indira Pradeepkumar.

ACKNOWLEDGMENTS

H. pylori strain 26695, graciously provided by Dr. Ashish Kumar Mukhopadhyay, National Institute of Cholera and Enteric Diseases (NICED), Kolkata. PY thanks the Science and Engineering Research Board, Department of Science and Technology, (SERB-DST, Grant No. ECR/2015/000431) for funding. VY research was supported by Department of Biotechnology, Government of India as Ramalingaswami Fellowship (BT/RLF/RE-ENTRY/29/2014); Indian Council of Medical Research (VIR/21/2022/ECD-I), Ministry of Education, Scheme for Transformational and Advanced Research in Sciences Grant (MoE-STARS/STARS-2/2023-0373); UGC-Start-up grant from University Grant Commission [30-553/2021 (BSR)]; The facilities/laboratories supported by DBT BUILDER (BT/INF/22/SP45382/2022) and DST FIST-II [SR/FST/LSII-046/2016(C)] to School of Life Sciences, Jawaharlal Nehru University, New Delhi.

CONFLICT OF INTEREST STATEMENT

The authors declare no conflicts of interest.

ORCID

Puja Yadav https://orcid.org/0000-0002-8650-9638

REFERENCES

1. Ceylan A, Kırımi E, Tuncer O, Türkdoğan K, Arıyuca S, Ceylan N. Prevalence of helicobacter pylori in children and their family members in a district in Turkey. J Health Popul Nutr. 2007;25(4):422–27. https://www.ncbi.nlm.nih.gov/pmc/articles/PMC2754017/
2. Graham DY, Adam E, Reddy GT, Agarwal JP, Agarwal R, Evans DJ, et al. Seroepidemiology of helicobacter pylori infection in India. Comparison of developing and developed countries. Dig Dis Sci. 1991;36(8):1084–88. https://doi.org/10.1007/BF01297451
3. Hooi JKY, Lai WY, Ng WK, Suen MMY, Underwood FE, Tanyingoh D, et al. Global prevalence of helicobacter pylori infection: systematic review and meta-analysis. Gastroenterology. 2017;153(2):420–29. https://doi.org/10.1053/j.gastro.2017.04.022
4. de Brito BB, da Silva FAF, Soares AS, Pereira VA, Santos MLC, Sampaio MM, et al. Pathogenesis and clinical management of helicobacter pylori gastric infection. World J Gastroenterol. 2019;25(37), 5578–89. https://doi.org/10.3748/wjg.v25.i37.5578
5. Mishra SK, Jain N, Shankar U, Tawani A, Sharma TK, Kumar A. Characterization of highly conserved G-quadruplex motifs as potential drug targets in *Streptococcus pneumoniae*. Sci Rep. 2019;9(1):1791. https://doi.org/10.1038/s41598-018-38400-x

6. Shankar U, Mishra SK, Jain N, Tawani A, Yadav P, Kumar A. Ni^{+2} permease system of Helicobacter pylori contains highly conserved G-quadruplex motifs. Infect Genet Evol. 2022;101:105298. https://doi.org/10.1016/j.meegid.2022.105298
7. Murat P, Balasubramanian S. Existence and consequences of G-quadruplex structures in DNA. Curr Opin Genet Dev. 2014;25:22–29. https://doi.org/10.1016/j.gde.2013.10.012
8. Rawal P, Kummarasetti VBR, Ravindran J, Kumar N, Halder K, Sharma R, et al. Genome-wide prediction of G4 DNA as regulatory motifs: role in *Escherichia coli* global regulation. Genome Res. 2006;16(5):644–55. https://doi.org/10.1101/gr.4508806
9. Shao X, Zhang W, Umar MI, Wong HY, Seng Z, Xie Y, et al. RNA G-quadruplex structures mediate gene regulation in bacteria. mBio. 2020;11(1):e02926-19. https://doi.org/10.1128/mBio.02926-19
10. Sun ZY, Wang XN, Cheng SQ, Su XX, Ou TM. Developing novel G-quadruplex ligands: from interaction with nucleic acids to interfering with nucleic acid⁻protein interaction. Molecules. 2019;24(3):396. https://doi.org/10.3390/molecules24030396
11. Yadav P, Kim N, Kumari M, Verma S, Sharma TK, Yadav V, et al. G-quadruplex structures in bacteria: biological relevance and potential as an antimicrobial target. J Bacteriol. 2021;203(13):e0057720. https://doi.org/10.1128/jb.00577-20
12. Yadav V, Hemansi, Kim N, Tuteja N, Yadav P. G quadruplex in plants: a ubiquitous regulatory element and its biological relevance. Front Plant Sci, 2017;8:1163. https://doi.org/10.3389/fpls.2017.01163
13. Kumari S, Bugaut A, Huppert JL, Balasubramanian S. An RNA G-quadruplex in the 5' UTR of the NRAS proto-oncogene modulates translation. Nat Chem Biol. 2007;3(4):218–21. https://doi.org/10.1038/nchembio864
14. Bauer L, Tlučková K, Tóhová P, Viglaský V. G-quadruplex motifs arranged in tandem occurring in telomeric repeats and the insulin-linked polymorphic region. Biochemistry. 2011;50(35):7484–92. https://doi.org/10.1021/bi2003235
15. Saad M, Guédin A, Amor S, Bedrat A, Tourasse NJ, Fayyad-Kazan H, et al. Mapping and characterization of G-quadruplexes in the genome of the social amoeba *Dictyostelium discoideum*. Nucleic Acids Res. 2019;47(9):4363–74. https://doi.org/10.1093/nar/gkz196
16. Saad M, Mehawej C, Faour WH. Analysis of G-quadruplex forming sequences in podocytes-marker genes and their potential roles in inherited glomerular diseases. Heliyon. 2023;9(9):e20233. https://doi.org/10.1016/j.heliyon.2023.e20233
17. Huppert JL, Balasubramanian S. Prevalence of quadruplexes in the human genome. Nucleic Acids Res. 2005;33(9):2908–16. https://doi.org/10.1093/nar/gki609
18. Largy E, Mergny JL, Gabelica V. Role of alkali metal ions in G-quadruplex nucleic acid structure and stability. Met Ions Life Sci. 2016;16:203–58. https://doi.org/10.1007/978-3-319-21756-7_7
19. Cueny RR, McMillan SD, Keck JL. G-quadruplexes in bacteria: insights into the regulatory roles and interacting proteins of non-canonical nucleic acid structures. Crit Rev Biochem Mol Biol. 2022;57(5–6):539–61. https://doi.org/10.1080/10409238.2023.2181310
20. Bugaut A, Balasubramanian S. A sequence-independent study of the influence of short loop lengths on the stability and topology of intramolecular DNA G-quadruplexes. Biochemistry. 2008;47(2):689–97. https://doi.org/10.1021/bi701873c
21. Kikin O, D'Antonio L, Bagga PS. QGRS Mapper: a web-based server for predicting G-quadruplexes in nucleotide sequences. Nucleic Acids Res. 2006;34(Web Server issue):W676–82. https://doi.org/10.1093/nar/gkl253
22. Eddy J, Maizels N. Gene function correlates with potential for G4 DNA formation in the human genome. Nucleic Acids Res. 2006;34(14):3887–96. https://doi.org/10.1093/nar/gkl529
23. Pathak R. G-quadruplexes in the viral genome: unlocking targets for therapeutic interventions and antiviral strategies. Viruses. 2023;15(11):2216. https://doi.org/10.3390/v15112216
24. Müller S, Rodriguez R. G-quadruplex interacting small molecules and drugs: from bench toward bedside. Expert Rev Clin Pharmacol. 2014;7(5):663–79. https://doi.org/10.1586/17512433.2014.945909
25. Anas M, Sharma R, Dhamodharan V, Pradeepkumar PI, Manhas A, Srivastava K, et al. Investigating pharmacological targeting of G-quadruplexes in the human malaria parasite. Biochemistry. 2017;56(51):6691–99. https://doi.org/10.1021/acs.biochem.7b00964
26. Lemarteleur T, Gomez D, Paterski R, Mandine E, Mailliet P, Riou JF. Stabilization of the c-myc gene promoter quadruplex by specific ligands' inhibitors of telomerase. Biochem Biophys Res Commun. 2004;323(3):802–8. https://doi.org/10.1016/j.bbrc.2004.08.150
27. Pennarun G, Granotier C, Gauthier LR, Gomez D, Hoffschir F, Mandine E, et al. Apoptosis related to telomere instability and cell cycle alterations in human glioma cells treated by new highly selective G-quadruplex ligands. Oncogene. 2005;24(18):2917–28. https://doi.org/10.1038/sj.onc.1208468
28. De Cian A, Delemos E, Mergny JL, Teulade-Fichou MP, Monchaud D. Highly efficient G-quadruplex recognition by bisquinolinium compounds. J Am Chem Soc. 2007;129(7):1856–57. https://doi.org/10.1021/ja067352b
29. Gomez D, Guédin A, Mergny JL, Salles B, Riou JF, Teulade-Fichou MP, et al. A G-quadruplex structure within the 5′-UTR of TRF2 mRNA represses translation in human cells. Nucleic Acids Res. 2010;38(20):7187–98. https://doi.org/10.1093/nar/gkq563
30. Yang D. G-quadruplex DNA and RNA. Methods Mol Biol. 2019;2035:1–24. https://doi.org/10.1007/978-1-4939-9666-7_1
31. Guédin A, Gros J, Alberti P, Mergny J-L. How long is too long? Effects of loop size on G-quadruplex stability. Nucleic Acids Res, 2010;38(21):7858–68. https://doi.org/10.1093/nar/gkq639
32. Tatusov RL, Galperin MY, Natale DA, Koonin EV. The COG database: a tool for genome-scale analysis of protein functions and evolution. Nucleic Acids Res. 2000;28(1):33–36. https://doi.org/10.1093/nar/28.1.33
33. Dhamodharan V, Harikrishna S, Jagadeeswaran C, Halder K, Pradeepkumar PI. Selective G-quadruplex DNA stabilizing agents based on bisquinolinium and bispyridinium derivatives of 1,8-naphthyridine. J Org Chem. 2012;77(1):229–42. https://doi.org/10.1021/jo201816g
34. Clinical and Laboratory Standards Institute (CLSI). Performance standards for antimicrobial susceptibility testing CLSI supplement M100. 33rd ed. Wayne: Clinical and Laboratory Standards Institute; 2023.
35. Mosmann T. Rapid colorimetric assay for cellular growth and survival: application to proliferation and cytotoxicity assays. J Immunol Methods. 1983;65(1–2):55–63. https://doi.org/10.1016/0022-1759(83)90303-4

36. Wang H, Cheng H, Wang F, Wei D, Wang X. An improved 3-(4,5-dimethylthiazol-2-yl)-2,5-diphenyl tetrazolium bromide (MTT) reduction assay for evaluating the viability of *Escherichia coli* cells. J Microbiol Methods. 2010;82(3):330–33. https://doi.org/10.1016/j.mimet.2010.06.014
37. Palermo EF, Kuroda K. Chemical structure of cationic groups in amphiphilic polymethacrylates modulates the antimicrobial and hemolytic activities. Biomacromolecules, 2009;10(6):1416–28. https://doi.org/10.1021/bm900044x
38. Xiao S, Zhang JY, Zheng KW, Hao YH, Tan Z. Bioinformatic analysis reveals an evolutional selection for DNA:RNA hybrid G-quadruplex structures as putative transcription regulatory elements in warm-blooded animals. Nucleic Acids Res. 2013;41(22):10379–90. https://doi.org/10.1093/nar/gkt781
39. Du Z, Zhao Y, Li N. Genome-wide analysis reveals regulatory role of G4 DNA in gene transcription. Genome Res. 2008;18(2):233–41. https://doi.org/10.1101/gr.6905408
40. Eddy J, Maizels N. Conserved elements with potential to form polymorphic G-quadruplex structures in the first intron of human genes. Nucleic Acids Res. 2008;36(4):1321–33. https://doi.org/10.1093/nar/gkm1138
41. Verma A, Halder K, Halder R, Yadav VK, Rawal P, Thakur RK, et al. Genome-wide computational and expression analyses reveal G-quadruplex DNA motifs as conserved cis-regulatory elements in human and related species. J Med Chem. 2008;51(18):5641–49. https://doi.org/10.1021/jm800448a
42. Zhao Y, Du Z, Li N. Extensive selection for the enrichment of G4 DNA motifs in transcriptional regulatory regions of warm blooded animals. FEBS Lett. 2007;581(10):1951–56. https://doi.org/10.1016/j.febslet.2007.04.017
43. Čutová M, Manta J, Porubiaková O, Kaura P, Šťastný J, Jagelská EB, et al. Divergent distributions of inverted repeats and G-quadruplex forming sequences in *Saccharomyces cerevisiae*. Genomics. 2020;112(2):1897–901. https://doi.org/10.1016/j.ygeno.2019.11.002
44. Bartas M, Čutová M, Brázda V, Kaura P, Šťastný J, Kolomazník J, et al. The presence and localization of G-quadruplex forming sequences in the domain of bacteria. Molecules. 2019;24(9):1711. https://doi.org/10.3390/molecules24091711
45. Sperandeo P, Martorana AM, Polissi A. Lipopolysaccharide biogenesis and transport at the outer membrane of Gram-negative bacteria. Biochim Biophys Acta Mol Cell Biol Lipids. 2017;1862(11):1451–60. https://doi.org/10.1016/j.bbalip.2016.10.006
46. Tanaka KJ, Song S, Mason K, Pinkett HW. Selective substrate uptake: the role of ATP-binding cassette (ABC) importers in pathogenesis. Biochim Biophys Acta Biomembr. 2018;1860(4):868–77. https://doi.org/10.1016/j.bbamem.2017.08.011
47. Thomas C, Tampé R. Multifaceted structures and mechanisms of ABC transport systems in health and disease. Curr Opin Struct Biol, 2018;51:116–28. https://doi.org/10.1016/j.sbi.2018.03.016
48. Furuta Y, Konno M, Osaki T, Yonezawa H, Ishige T, Imai M, et al. Microevolution of virulence-related genes in *Helicobacter pylori* Familial Infection. PLoS ONE. 2015;10(5):e0127197. https://doi.org/10.1371/journal.pone.0127197
49. Yang F, Zhang J, Wang S, Sun Z, Zhou J, Li F, et al. Genomic population structure of *Helicobacter pylori* Shanghai isolates and identification of genomic features uniquely linked with pathogenicity. Virulence. 2021;12(1):1258–70. https://doi.org/10.1080/21505594.2021.1920762
50. Kumar N, Mariappan V, Baddam R, Lankapalli AK, Shaik S, Goh KL, et al. Comparative genomic analysis of *Helicobacter pylori* from Malaysia identifies three distinct lineages suggestive of differential evolution. Nucleic Acids Res. 2015;43(1):324–35. https://doi.org/10.1093/nar/gku1271
51. Ivain L, Bordeau V, Eyraud A, Hallier M, Dreano S, Tattevin P, et al. An in vivo reporter assay for sRNA-directed gene control in gram-positive bacteria: identifying a novel sRNA target in *Staphylococcus aureus*. Nucleic Acids Res. 2017;45(8):4994–5007. https://doi.org/10.1093/nar/gkx190
52. Wang W, Ma Y, He J, Qi H, Xiao F, He S. Gene regulation for the extreme resistance to ionizing radiation of *Deinococcus radiodurans*. Gene. 2019;715:144008. https://doi.org/10.1016/j.gene.2019.144008
53. Nester EW, Jensen RA. Control of aromatic acid biosynthesis in *Bacillus subtilis*: sequenial feedback inhibition. J Bacteriol. 1966;91(4):1594–98. https://doi.org/10.1128/jb.91.4.1594-1598.1966
54. Goelzer A, Bekkal Brikci F, Martin-Verstraete I, Noirot P, Bessières P, et al. Reconstruction and analysis of the genetic and metabolic regulatory networks of the central metabolism of *Bacillus subtilis*. BMC Syst Biol. 2008;2:20. https://doi.org/10.1186/1752-0509-2-20
55. Matta AJ, Zambrano DC, Martínez YC, Fernández FF. Point mutations in the glycosyltransferase domain of the pbp1a gene in amoxicillin-resistant *Helicobacter pylori* isolates. Rev Gastroenterol Mex (English). 2023;88(2):100–106. https://doi.org/10.1016/j.rgmxen.2021.05.015
56. Tran TT, Nguyen AT, Quach DT, Pham DTH, Cao NM, Nguyen UTH, et al. Emergence of amoxicillin resistance and identification of novel mutations of the pbp1A gene in *Helicobacter pylori* in Vietnam. BMC Microbiol. 2022;22(1):41. https://doi.org/10.1186/s12866-022-02463-8
57. Alka K, Windle HJ, Cornally D, Ryan BJ, Henehan GTM. A short chain NAD(H)-dependent alcohol dehydrogenase (HpSCADH) from *Helicobacter pylori*: a role in growth under neutral and acidic conditions. Int J Biochem Cell Biol. 2013;45(7):1347–55. https://doi.org/10.1016/j.biocel.2013.04.006
58. Silva LDC, Silva KSFE, Rocha OB, Barbosa KLB, Rozada AMF, Gauze GF, et al. Proteomic response of *Paracoccidioides brasiliensis* exposed to the antifungal 4-methoxynaphthalene-*N*-acylhydrazone reveals alteration in metabolism. J Fungi (Basel, Switzerland). 2022;9(1):66. https://doi.org/10.3390/jof9010066

SUPPORTING INFORMATION

Additional supporting information can be found online in the Supporting Information section at the end of this article.

How to cite this article: Kumari M, Jaiswal S, Shankar U, Gupta S, Pradeepkumar P, Kumar A, et al. Characterization of G-quadruplexes in the *Helicobacter pylori* genome and assessment of therapeutic potential of G4 ligands. Biotechnol Appl Biochem. 2024;:e2644. https://doi.org/10.1002/bab.2644